Available online at www.sciencedirect.com
SCIENCE DIRECT®

Precision Engineering 29 (2005) 41–47

PRECISION ENGINEERING

www.elsevier.com/locate/precision

Dimensionless design graphs for flexure elements and a comparison between three flexure elements

Wouter O. Schotborgh, Frans G.M. Kokkeler*, Hans Tragter, Fred J.A.M. van Houten

Laboratory of Design, Production and Management, Department of Mechanical Engineering, University of Twente, P.O. Box 217, 7500 AE Enschede, The Netherlands

Received 16 May 2003; received in revised form 31 March 2004; accepted 21 April 2004
Available online 19 June 2004

Abstract

This paper presents dimensionless design graphs for three types of flexure elements, based on finite element analysis. Using these graphs as a design tool, a designer can determine the optimal geometry, based on the stiffness and rotation demands of a flexure element. An example is given using the beam flexure hinge.

Between the analyzed flexure hinges, a comparison is made on basis of equal hinge functionality: rotation. The result describes the maximum stiffness properties from different hinges in identical situations. A beam flexure element is preferred over a circular flexure hinge for stiffness demands in a single direction, while a cross flexure element enables medium stiffness in two perpendicular directions.

Keywords: Flexure hinge; Design tool; Design graph; Circular hinge; Beam hinge; Cross hinge; Comparison

1. Introduction

As miniaturization continues in many fields of modern technology, the demand for precision mechanisms increases with it. One specific kind of precision mechanisms is called ‘compliant mechanisms’, as discussed by Howell [1] and Smith [2]. These mechanisms are widely used where high accuracy is demanded over a short range of motion.

The compliant mechanism uses ‘flexure hinges’ in order to introduce local rotational degrees of freedom into the mechanism. A flexure element rotates as a result of local elastical deformation, as shown in Fig. 1. The describing parameters and coordinate system are also presented in the figure.

Although flexure hinges provide only a limited rotation angle, there are definite benefits above sliding or rolling hinges: rotation without friction losses, lubrication, hysteresis or maintenance. Being monolithic with the rest of the mechanism for the vast majority of applications, this results in low production costs and virtually no assembly, according to Howell [1].

For this paper, only monolithic flexure elements are taken into account, for use in two-dimensional mechanisms. These mechanisms, including the hinge points, can be manufactured by wire electro-discharge machining. The three types which are handled in this paper are shown in Fig. 2.

In Fig. 1, the relevant coordinate system and parameters of a circular hinge are shown. Important design properties for any type of flexure hinge are stiffness in rotation direction ψ, stiffness in x- and z-direction and the stress build up due to bending (elastic deformation) over an angle ψ. Also stresses which result from normal forces N, including the stress concentration factor as a result of the shape of the hinge, have to be taken into account. For a circular hinge, a dimensionless design graph has been constructed several decades ago and presented by Koster [3]. This graph is reproduced in this paper to ensure consistency.

These graphs are constructed using finite element calculations. Smith states [4] that this data can be assumed to be the ‘true’ stiffness behaviour.

Beside the choice of the *type* of flexure element, the *geometry* itself determines the important properties of the flexure hinge like stiffness and allowed rotation angle.

In this paper, the relationship between geometry and hinge behaviour are presented both numerically and graphically, to assist the designer in the process of choosing both the type of hinge and the geometry during the first stages of the design process.

* Corresponding author. Fax: +31-53-4893631.
E-mail address: F.G.M.Kokkeler@utwente.nl (F.G.M. Kokkeler).

0141-6359/$ – see front matter © 2004 Published by Elsevier Inc.
doi:10.1016/j.precisioneng.2004.04.003

Nomenclature

C	stiffness
D	circular shape diameter
E	Young's modulus
F	force
h	flexure hinge thickness parameter
k	rotation stiffness
L	flexure hinge beam length parameter
N	normal force
t	plate thickness
T	bending moment
x,y,z	reference axes
ν	Poisson ratio
γ	form factor for shear deformation = 6/5 [5]

Greek symbols

σ	stress
φ,ψ,θ	reference rotations

Subscripts

x,y,z	reference axes
φ,ψ,θ	reference rotations

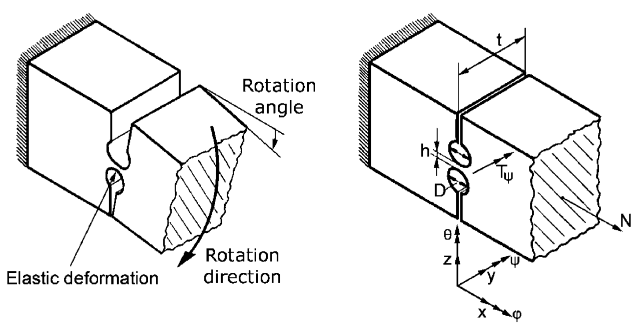

Fig. 1. Flexure element.

2. The circular hinge

The dimensionless design graph for the circular flexure hinge is reproduced using the finite element calculations program ANSYS. For these calculations, the geometry of the 3D hinge is modelled using a 2D quarter of the model, shown in Fig. 3.

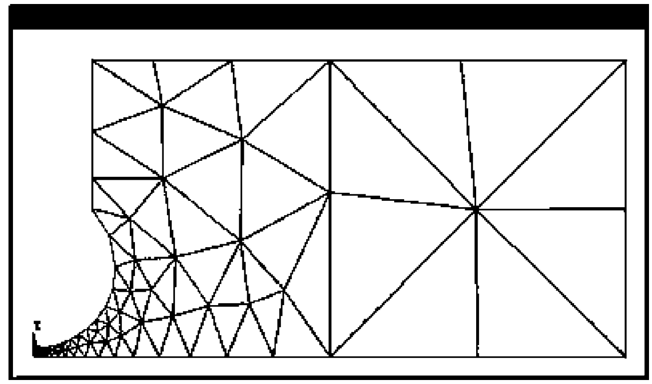

Fig. 3. Circular hinge model.

In this model, thickness is not taken into account separately, but included by using the element type plane stress (small thickness relative to the radius) or plane strain (large thickness). In this case, plane stress elements are used because this results in the safe situation of 5–10% under estimation of the stiffness in x-, z- and ψ-direction, rather than a possible over estimation.

The stress data itself is not affected by the choice for plane stress elements, because a constant torque has been applied to study stress due to rotation.

The most important aspects of the finite element programming can be summarized:

- ANSYS version: 6.1.
- Element type: Plane2, a 6-node triangular element with quadratic displacement behaviour. This type is well suited for meshing of irregular shapes. The element is used in this application as plane stress element.
- Material properties: The Young's modulus used is that of steel: 210×10^9 Pa. The Poisson's ratio used is 0.28.

In order to characterize the flexure hinge more mathematically, the large number of data points (25 per graph line) are fitted with a function. In this case, the equations of the lines are formed by second order polynomial fitting, using the least square method.

The order of the polynomial function is chosen to be two for the circular hinge, since fitting the data points with higher order polynomials results in a marginal improvement of the norm of residuals, compared to the 5–10% under estimation of the values themselves.

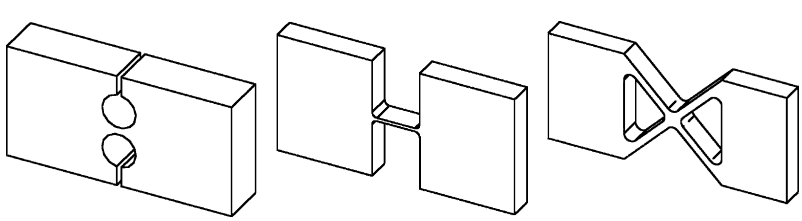

Fig. 2. Flexure elements.

For a circular hinge, as shown in Fig. 1, the equations for the dimensionless numbers are given below.

Dimensionless stiffness in x-direction C_{xx} (1):

$$\frac{C_{xx}}{E \times t} = 0.0010 + 0.4256\sqrt{\frac{h}{D}} + 0.0824\left(\sqrt{\frac{h}{D}}\right)^2 \quad (1)$$

Dimensionless stiffness in z-direction C_{zz} (2):

$$\frac{C_{zz}}{E \times t} = 0.0040 - 0.0727\sqrt{\frac{h}{D}} + 0.3417\left(\sqrt{\frac{h}{D}}\right)^2 \quad (2)$$

Dimensionless rotation stiffness $k_{\psi\psi}$ (3):

$$\frac{12 \times k_{\psi\psi}}{E \times t \times h^2} = -0.0089 + 1.3556\sqrt{\frac{h}{D}} - 0.5227\left(\sqrt{\frac{h}{D}}\right)^2 \quad (3)$$

Dimensionless rotation stress $\sigma_{\psi\psi}$ (4):

$$\frac{\sigma_{\psi\psi}}{\psi \times E} = -0.0028 + 0.6397\sqrt{\frac{h}{D}} - 0.0856\left(\sqrt{\frac{h}{D}}\right)^2 \quad (4)$$

Dimensionless stress concentration σ_x due to normal force N (5):

$$\frac{\sigma_x \times h \times t}{N} = 0.9951 + 0.0542\sqrt{\frac{h}{D}} + 0.5171\left(\sqrt{\frac{h}{D}}\right)^2 \quad (5)$$

The equations describe the stiffness for a circular hinge directly as a function of the geometry, as represented graphically in Fig. 4. The use of the square root is merely to enlarge the clarity of the graph for the smaller h/D ratios, which are most realistic for practical use.

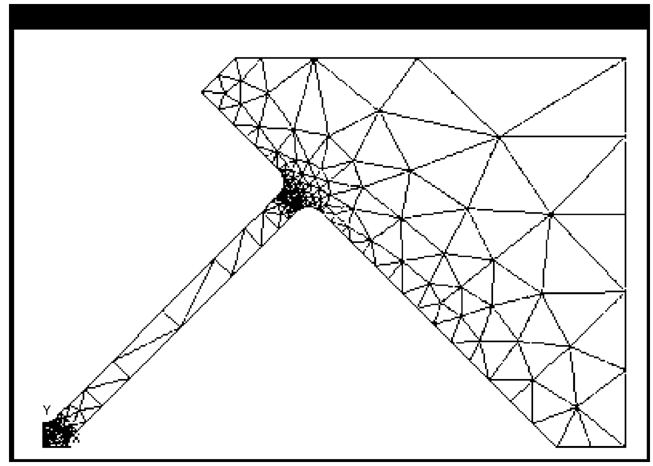

Fig. 5. Cross hinge model.

3. The cross hinge

Similar to the circular hinge graph, a design graph is constructed for the cross hinge using finite element calculations. Modeling again one 2D quarter of the actual geometry, identical load cases have been subjected to this model. The geometry and model used is shown in Fig. 5. In order to have reliable information concerning the stress behaviour, the mesh is refined at the locations where the stress concentrations are expected: around the fillets.

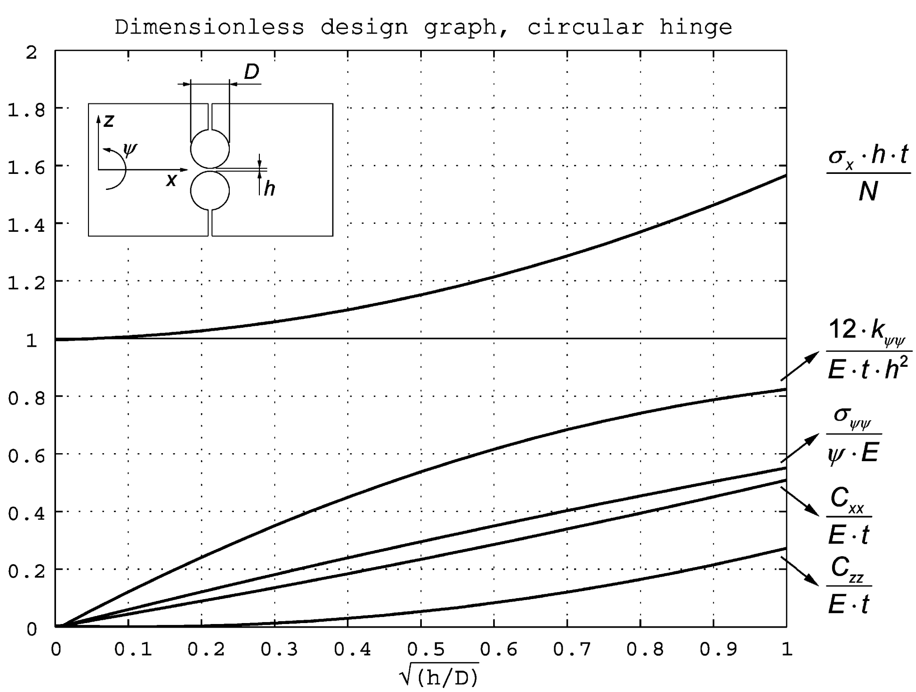

Fig. 4. Dimensionless design graph for circular hinge.

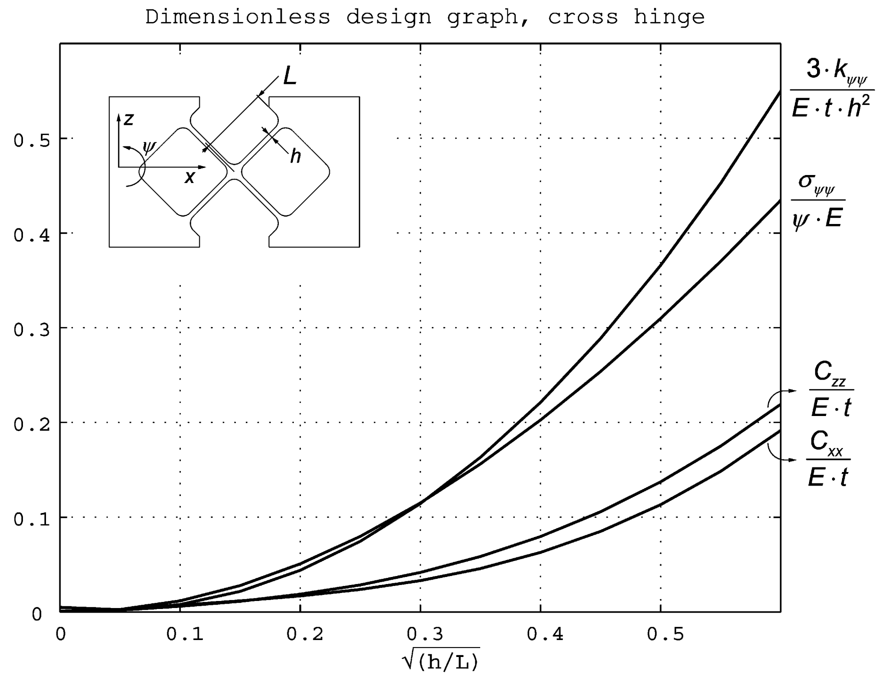

Fig. 6. Dimensionless design graph for cross hinge.

The fillet radius is taken 70% of the beam thickness, since this is the optimal value for bending beams, as explained later in this paper.

As with the circular hinge graph, a dimensionless design graph is constructed for the cross hinge, shown in Fig. 6.

The equations of these lines are formed by third order polynomial functions, using the same motivation as the circular hinge fitting, where an increase in polynomial order does not lead to a significantly higher accuracy.

The equations for the dimensionless numbers are:

Dimensionless stiffness in x-direction C_{xx} (6):

$$\frac{C_{xx}}{E \times t} = -0.0033 + 0.1333\sqrt{\frac{h}{L}} - 0.3984\left(\sqrt{\frac{h}{L}}\right)^2 + 1.1962\left(\sqrt{\frac{h}{L}}\right)^3 \quad (6)$$

Dimensionless stiffness in z-direction C_{zz} (7):

$$\frac{C_{zz}}{E \times t} = -0.0012 + 0.0590\sqrt{\frac{h}{L}} + 0.0434\left(\sqrt{\frac{h}{L}}\right)^2 + 0.7850\left(\sqrt{\frac{h}{L}}\right)^3 \quad (7)$$

Dimensionless rotation stiffness $k_{\psi\psi}$ (8):

$$\frac{3 \times k_{\psi\psi}}{E \times t \times h^2} = 0.0048 - 0.1289\sqrt{\frac{h}{L}} + 1.5663\left(\sqrt{\frac{h}{L}}\right)^2 + 0.2704\left(\sqrt{\frac{h}{L}}\right)^3 \quad (8)$$

Dimensionless rotation stress $\sigma_{\psi\psi}$ (9):

$$\frac{\sigma_{\psi\psi}}{\psi \times E} = 0.0009 - 0.0418\sqrt{\frac{h}{L}} + 1.5426\left(\sqrt{\frac{h}{L}}\right)^2 - 0.4463\left(\sqrt{\frac{h}{L}}\right)^3 \quad (9)$$

The stress concentration factor [5] for forces acting on the hinge is not represented separately in the graph, since the fillet radius is given a fixed value resulting in a constant factor of about 1.4.

4. The beam hinge

Since it is relatively straight forward to analyze the stiffness and stress behaviour of a beam, no finite element calculations are made to construct the design graph for this type of flexure hinge. Instead, the graph is directly derived from the stress and stiffness formulas of Bernoulli beams, as stated by Gere and Timoshenko [5]. The coordinate system and dimensions are shown in Fig. 7.

The stiffness C_{xx} in length direction of a beam (10):

$$C_{xx} = \frac{E \times t \times h}{L} \quad (10)$$

The stiffness C_{zz} perpendicular to the length direction of a beam (11):

$$C_{zz} = \frac{E \times t \times h^3}{L^3 + 2\gamma(1 + \upsilon)L \times h^2} \quad (11)$$

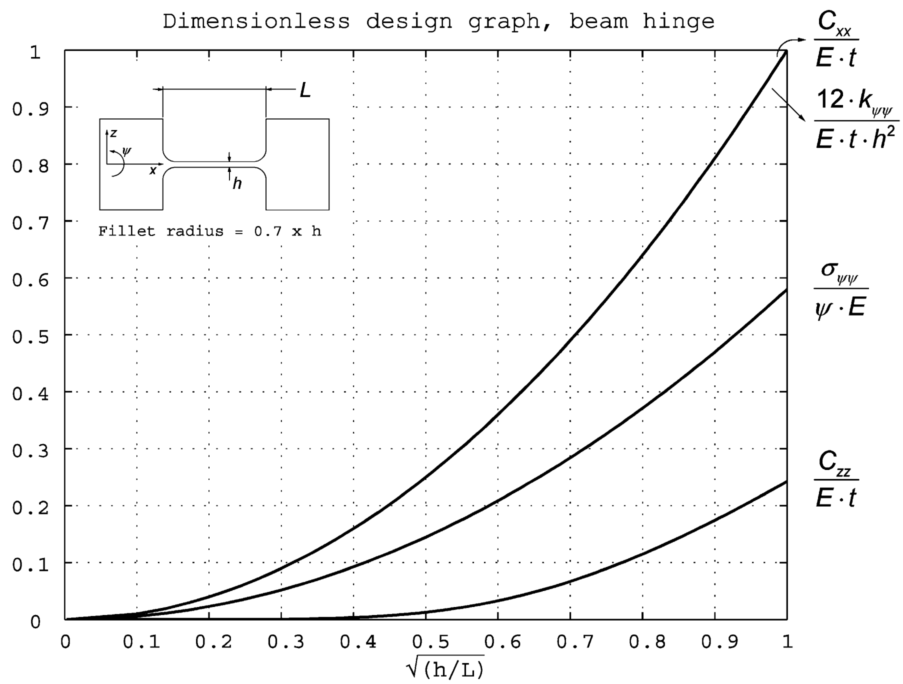

Fig. 7. Dimensionless design graph for beam hinge.

where γ is the compensation factor for shear deformation [5], and υ is the Poisson ratio [5].

The theoretical rotation stiffness $k_{\psi\psi}$ of a beam (12):

$$k_{\psi\psi} = \frac{E \times t \times h^3}{12 \times L} \tag{12}$$

The rotation stress $\sigma_{\psi\psi}$ due to bending of an ideal beam (13):

$$\sigma_{\psi\psi} = \frac{\psi \times E \times h}{2 \times L} \tag{13}$$

Because the flexure element is attached to relatively stiff elements, stress concentration due to a fillet radius is present. In order to have the optimal fillet radius, the occurring stress concentration factor should be as low as possible, however still allowing for good rotation.

Consider a beam flexure attached to the fixed world, while the free end is under constant torque: a too large fillet radius introduces only little stress concentration, but also little rotation because it stiffens the beam. A too small radius results in higher rotation, but introduces a large stress concentration.

The optimal situation is that which results in lowest stress concentration relative to the highest rotation.

After finite element analysis over a wide range of different radii, the optimal fillet radius is found to be 70% of the beam height. This results in a 16% increase of dimensionless rotation stress, compared to an ideal beam without connection to the fixed world. Thus, formula (13) can be compensated for this, resulting in (14):

$$\sigma_{\psi\psi} = \frac{\psi \times E \times h}{2 \times L} \times 1.16 \tag{14}$$

where 1.16 is the fillet radius influence, for a radius of 0.7 h.

For forces acting on the beam, this fillet radius results in a stress concentration factor of about 1.4.

The effect it has on the stiffness in *x*- and *z*-direction is neglected, since it is expected to have only a minor (positive) effect.

With the above stated formulas, the dimensionless design graph for beam flexures can be constructed as shown in Fig. 7. The *x*-axis represents the $\sqrt{h/L}$ value, to give visual comparison with the other design graphs. The dimensionless rotation stress is compensated with the fillet radius influence, using Eq. (14).

5. Use of the design graph

The dimensionless design graph combines the geometry of the hinge with its functional characteristics. This is done through dimensionless numbers at the vertical axis. For beam flexures this can be seen in Fig. 7.

An example calculation:

Consider a beam flexure which rotates from -0.035 to $+0.035$ rad (total angle 4.0°). Using 42CrMo4 steel [DIN17200], the allowed stress level is 600×10^6 N/m^2 and the Young's modulus is 210×10^9 N/m^2. The dimensionless number for rotation stress now becomes (15):

$$\frac{\sigma_{\psi\psi}}{\psi \times E} = 0.08 \tag{15}$$

The corresponding geometrical constraint for the beam flexure hinge is found from the graph, or Eqs. (10)–(14), to be $\sqrt{(h/L)} = 0.38$. The resulting stiffness in *x*- and *z*-direction, for a 10 mm material thickness, can be derived directly: 3.0×10^8 and 6.3×10^6 N/m, respectively.

These stiffness values can be compared to the desired situation, as commonly derived from dynamic performance specifications of the mechanism. For a higher stiffness, or better dynamic performance, concessions have to be made regarding the rotation angle, the allowed stress or the plate thickness. This relation is described in the following formula (16) for stiffness in *x*-direction:

$$C_{xx} = \frac{\sigma_{\psi\psi} \times t \times 1.72}{\psi} \tag{16}$$

If an acceptable stiffness is found, the only remaining parameter is height '*h*'. For this value, the minimum manufactu-

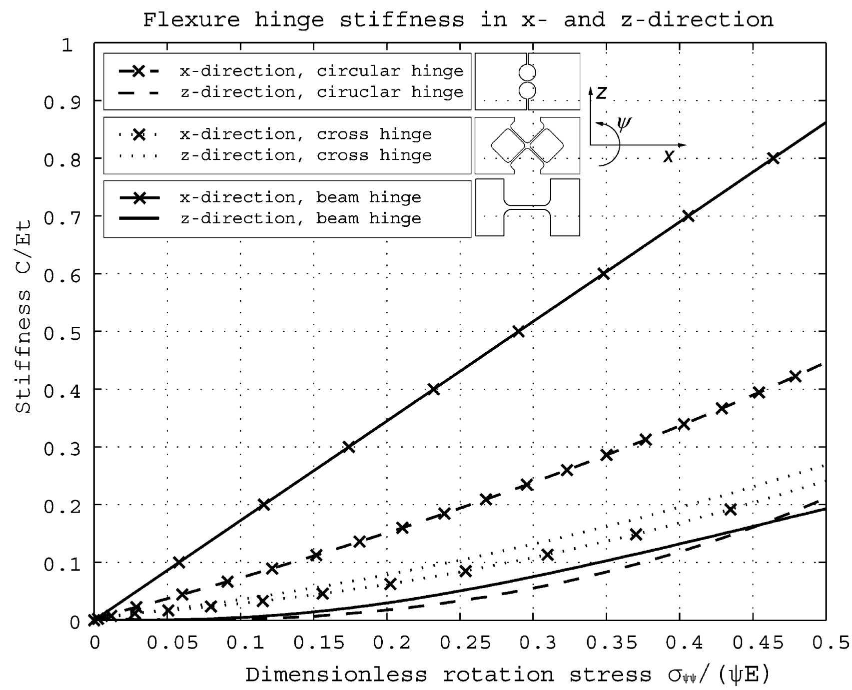

Fig. 8. Comparison stiffness in *x*- and *z*-direction.

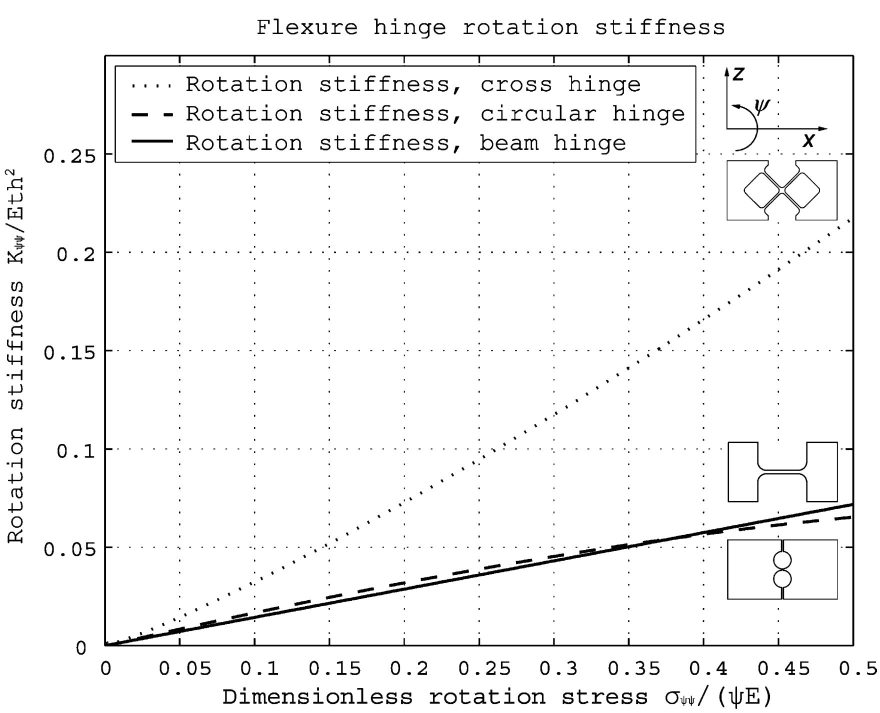

Fig. 9. Comparison rotation stiffness.

ring height can be taken; 0.3 mm. The rotation stiffness can now be derived: $k_{\psi\psi} = 2.3$ Nm/rad. This value can be used to calculate the force which the actuator is required to deliver.

The designed flexure hinge has a height of 0.3 mm and a length of 2.1 mm, with fillet radius 0.21 mm.

6. Comparison

Now that the three flexure types are analyzed, it is possible to make a comparison and determine the most favorable.

Instead of comparing on the basis of equal geometry, as done by Lobontiu et al. [6] and Xu and King [7], the hinges are compared on the basis of *function*: equal rotation angle. The question then is; which type has the highest possible stiffness in *x*- and *z*-direction, at equivalent stress levels.

Consider a flexure being rotated over a certain angle ψ. Regardless of the type of hinge, the material allows only a certain stress $\sigma_{\psi\psi}$ to do so. From the rotation angle, material property and allowed stress, a value for the dimensionless rotation stress is found (15):

$$\frac{\sigma_{\psi\psi}}{\psi \times E} = 0.08 \tag{15}$$

As shown in the foregoing section, this leads to a specific stiffness in *x*- and *z*-direction. For the three flexure types, these values can be compared visually by plotting them against the dimensionless rotation stress (hinge function), as is done in Fig. 8. The dimensionless stiffness is represented on the vertical axis, and the dimensionless rotation stress against the horizontal axis.

The same comparison is possible for the *rotation* stiffness. The three types are again compared on basis of equal rotation function. Now, the dimensionless rotation stiffness is plotted against the dimensionless rotation stress, thus leading to Fig. 9. The exact value of the rotation stiffness remains dependent on hinge parameter ‘*h*’. This is of course a different parameter for the circular-, beam- and cross hinge.

7. Conclusion

For circular-, cross- and beam flexure hinges, dimensionless design graphs are constructed which relate the stress-, stiffness- and rotation properties directly to the geometry. Using these graphs, the designer can determine the geometry of a flexure hinge based on the design demands.

In this paper, the attention is focused on the stress- and stiffness behaviour of flexure elements.

Based on the design graphs, a comparison is drawn between the properties of the flexure elements, when compared on basis of identical function: equal rotation angle and stress. This is visualized in Fig. 8. From this, several conclusions are drawn:

- A beam flexure element with specific fillet radius (0.7 × beam height) has two times higher stiffness in *x*-direction compared to a circular flexure hinge. The stiffness in *z*-direction is 10% higher for the majority of geometries.
- A cross flexure element is preferred above a beam flexure when stiffness in *z*-direction is absolutely demanded, however significant loss *x*-direction stiffness is inevitable.
- A comparison based on equal rotation function is performed with respect to the rotation stiffness: a beam hinge is equally stiff in rotation as a circular hinge. A cross hinge is twice as stiff in rotation as both circular- and beam flexure hinge.
- Based on stress- and stiffness analysis, a beam hinge is preferred over a circular hinge.
- A superior hinge can be constructed by a symmetrical ‘out of plane’ cross configuration of two perpendicular beam- or leaf elements, as shown in Fig. 10. Although this hinge is not easily manufactured by wire electro-discharge machining, it would result in maximum stiffness in both *x*- and *z*-direction. In the figure, solid bodies A and B can rotate relative to each other with optimal stiffness in all directions. This type can also be used in micro- and nano mechanism, since it can be manufactured by lithography. Using multiple layers, it is possible to produce a symmetrical cross configuration of beams which do not touch each other.

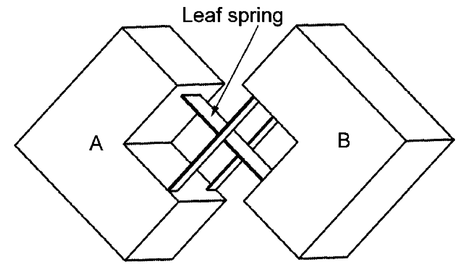

Fig. 10. Crossed leaf configuration.

With the above stated considerations and design aids, the design process of compliant mechanisms will be reduced in both time and complexity. The designer is able to determine the optimal geometry of the flexure hinges, based on the demands. This will speed up the design process significantly, leading to better designs with higher specifications.

References

[1] Howell LL. Compliant mechanisms. Wiley; 2001.
[2] Smith ST. Flexures: elements of elastic mechanisms. Gordon Breach Sci. Publ.; 2000.
[3] Koster MP. Constructieprincipes. Twente University Press; 2000.
[4] Smith ST. Elleptical flexure hinges. American Institute of Physics; 1997.
[5] Gere, Timoshenko. Mechanics of materials. Chapman & Hall; 1991.
[6] Lobontiu N, et al. Parabolic and hyperbolic flexure hinges: flexibility, motion precision and stress characterization based on compliance closed-form equations. Elsevier Science Inc.; 2002.
[7] Xu W, King T. Flexure hinges for piezoactuator displacement amplifiers: flexibility, accuracy and stress considerations. Elsevier Science Inc.; 1996.